Journal of Materials Science: Materials in Electronics (2020) 31:12083–12088
https://doi.org/10.1007/s10854-020-03753-5

Gold nanoparticles functionalized with 4,4′-dithiobiphenyl blended with CuS in PMMA for switching memory devices

Sara Cerra[1] · Paride Pica[1] · Mirko Congiu[1,2] · M. H. Boratto[2] · C. F.O. Graeff[2,3] · Ilaria Fratoddi[1]

Received: 4 February 2020 / Revised: 22 May 2020 / Accepted: 7 June 2020 / Published online: 12 June 2020

Abstract
A switching memory device based on functionalized gold nanoparticles (AuNPs) and hexagonal copper sulfide nanocrystals (CuS), finely blended in polymethylmethacrylate matrix (PMMA), is herein presented. A two-electrode sandwich architecture has been implemented using aluminum top and bottom electrodes and a polymeric insulating layer based on PMMA/AuNPs/CuS. The device showed memory storage capabilities suitable for (Read Only Memory) ROM applications and behaves as a typical Write-Once, Read-Many-times (WORM) device. The results obtained with the blend containing AuNPs and/or CuS were compared with pure PMMA. By a voltage ramp in the range ± 9 V, it was possible to permanently change the electrical resistance between the electrodes yielding an ON/OFF current ratio above 10^5 with long-term stability over the whole experiment duration (30 days).

1 Introduction

New-generation memory storage devices represent an important issue of modern research focused on artificial intelligence and neural networking, with a growing interest in the research of new materials and device structures. In this direction, several novel technologies have been studied and discussed so far in the literature, such as memory resistors (MEMs) and Write-Once, Read-Many-times memories (WORM) [1]. Historically, MEMs have been known as "the missing elements" in the theory of circuits, capable to fill the missing relationship between the charge *Q(t)* and the current flux *J(t)* [2]. This element remained a theoretical object until 2008 when it was fabricated for the first time by Hewlett-Packard labs [3]. Basically, MEMs are switchable resistors which can be set and reset by applying square voltage pulses [4]. Such devices are gaining huge interest in different areas of modern technology such as memory storage [5, 6], computing and logic operations [7, 8], neuromorphic computing applications [9, 10] and analog circuits [11]. There are two conductance states in memristors: higher resistance state (HRS), and low resistance state (LRS), also defined as R_{OFF} and R_{ON}, respectively. This way the device can be used as a Boolean logic switch returning (0) at HRS, R_{OFF}, and (1) at LRS, R_{ON} [7]. Along with MEMs, WORMs represent a class of new-generation memory devices. Basically, a WORM is a two-terminal device with an insulating film, HRS or R_{OFF}, between two metallic electrodes. The information can be written and recorded by applying a voltage pulse which induces the formation of a stable conductive channel, LRS or R_{ON}, between the two electrodes [12, 13]. The non-volatile character of WORM memories ensures the information recorded can be read many times [1, 14]. The research on new storage medium with improved performances is one of the goals of recent literature. The use of different semiconducting matrix has been exploited and the use of blends based on polymers and nanoparticles represents one of the most studied [15, 16]. Typically, an increase in the conduction of the devices is observed in the presence of metallic NPs and the conduction mechanism has been studied as a hopping between metallic NPs [17, 18]. There are still many open questions on the conduction process and on the effects on the performance due to parameters like size and materials choice, and among others gold NPs (AuNPs) have attracted much attention also in this field, due to their tunable functionalization and semiconducting properties

✉ Mirko Congiu
mirko.congiu@uniroma1.it

[1] Department of Chemistry, University of Rome Sapienza, P.le A. Moro 5, I-00185 Rome, Italy

[2] POSMAT – Post-Graduate Program in Materials Science and Technology, School of Sciences, UNESP – São Paulo State University, 17033-360 Bauru, SP, Brazil

[3] Department of Physics, School of Sciences, UNESP – São Paulo State University, 17033-360 Bauru, SP, Brazil

[19] that can be modified also by interconnection between particles, forming covalent NPs arrays and networks [20]. The fine dispersion of nanoparticles and homogeneity of the resulting blends are crucial to obtain reproducible results and considering this request, the clustering of nanoparticles can be avoided with a rigid linker between NPs. Different approaches have been addressed, so far in the literature, to enhance the physicochemical characteristics of self-assembled metallic nanoparticles networks using polymers as capping agent such as poly-ortho-toluidine (Au and Pd) [21]. A similar effect can be obtained also using multiwalled carbon nanotubes to cover the surface of noble metal nanoparticles [22, 23] and cuprous oxide [24].

In the present research, we investigated the application of gold nanoparticles (AuNPs) synthesized using 4,4'-dithiobiphenyl (BI) as ligand, and copper sulfide (CuS) that is a prominent material for switching memory devices [25, 26], in a polymeric matrix of Polymethylmethacrylate (PMMA). The combination of metallic nanoparticles (MNPs) with a narrow-gap semiconducting material such as CuS applied to memories can lead to enhanced electronic characteristics. As recently reported, the application of CuS/$Cu_{2-x}S$, a low-cost materials, as storage layer in random access memory (ReRAM) showed outstanding memristive characteristics [25]. Furthermore, the use of small concentrations of NPs embedded in a low-cost polymeric matrix deposited by non-vacuum methods objects the reduction of final cost of operating devices. In the present work, the study of a blend of PMMA, BI-capped AuNPs (AuNPs-BI) and CuS nanocrystals deposited by spin-coating and its application as the storage layer in WORM memories is reported.

2 Materials and methods

Anhydrous solvents were purchased from Sigma-Aldrich Co.: Dichloromethane (DCM), Ethanol, Toluene. Other solvents: N,N-Dimethylformamide (99,8%) from Synth, Isopropyl alcohol (99,77%) from Neon, Acetone (99,5%) from Dinâmica, deionized water (Milli-Q, 18.2 MΩ·cm). Reagents were purchased from Sigma-Aldrich Co.: 4,4'-dithiobiphenyl (BI) (95%), Tetrachloroauric (III) acid trihydrate ($HAuCl_4 \cdot 3H_2O$) (99.9%), Tetraoctylammonium bromide (TOAB) (99%), Sodium borohydride ($NaBH_4$) (99%); Polymethylmethacrylate (PMMA MW ~ 15000 u.m.a.) from Synth-Brazil; and glass substrate from Precision. Current versus voltage (IV) curves were registered using Keithley 2400C and our custom software (Mem wizard) [27]. The cyclic voltammetry measurements were performed in the range ± 9 V in both blank and employed samples. AuNPs-BI synthesis was carried out starting from Tetrachloroauric (III) acid trihydrate with a well-assessed wet reduction procedure [28, 29], with the Au:BI molar ratio equal to 4:1. Briefly, 108 mg (2.7×10^{-4} mmol) of $HAuCl_4$ was dissolved in 5 mL of H_2O_{up} and transferred in a 100 mL two-neck round bottom flask. Subsequently, 2.8×10^{-4} mmol of TOAB dissolved in 10 mL of toluene was added, as the phase-transfer reagent. The two-phase water/toluene mixture was vigorously stirred for 10 min, until complete transfer of the $AuCl_4^-$ anion had occurred. Then, 13.3 mg (6.1×10^{-5} mmol) of the bifunctional capping agent 4,4'-dithiobiphenyl dissolved in 10 mL of toluene was added to the previous mixture under N_2 flux. A freshly prepared aqueous solution of $NaBH_4$ (2.6×10^{-3} mmol; 5 mL H_2O_{up}) was added dropwise. On addition of the reducing agent, the organic phase changes color from orange to deep brown within a few seconds. After being stirred for 3 h at room temperature, the organic phase was separated with a separatory funnel, evaporated to 2 mL in a rotary evaporator, mixed with 40 mL ethanol and then kept in a refrigerator at −18 °C overnight. The mixture was centrifuged 10 times (13400 rpm, 10 min) to remove excess thiol. The resulting dark precipitate was dried in a rotary evaporator and stored for further use. Yield: 31 ± 4%.

Hexagonal CuS nanocrystals were prepared following the method proposed by Basu et al. [30]. The PMMA//AuNPs-BI/CuS blend was prepared as follows: a solution of PMMA in DCM (100 mg/mL) was prepared by mixing the powdered polymer with the solvent in a vial during constant magnetic stirring at 60 °C. When the polymer was completely dissolved (after 2 h), the obtained solution was filtered with a 0.20 µm pore filter (Millipore). In another vial, 40 mg/mL of CuS was dissolved in pure DMF at 60 °C, and then 40 mg/mL of AuNPs-BI was added to the mixture under vigorous stirring. The as-obtained slurry suspension was mixed with the PMMA solution to obtain a final concentration of 5 mg/mL of both CuS and AuNPs-BI corresponding to a concentration of ~ 5% (4.76%) in the dry film. The slurry was sonicated up to 30 min before use.

Al bottom electrode was deposited on clean glass substrate (1.5 × 2.0 cm) by resistive evaporation using shadow-mask at low pressure of about 3×10^{-5} Torr using an Auto500 System (Edwards). Then an aliquot of the PMMA/AuNPs-BI/CuS) slurry (200 µL) was directly spin-coated on top of the substrate electrode using a WS-400B-6NPP/LITE (Laurell) at 4000 rpm for 60 s. After the spin-coating process, Al electrodes were evaporated on the top layer creating a crossbar configuration, with an area of 4 mm^2 (Figure 1).

Electrical characterization through current versus voltage (I vs. V) curves was registered using Keithley 2400C coupled to a computer. The cyclic voltammetry (CV) measurements were performed in the range ± 9 V in both blank and working samples. The values of R_{ON} and R_{OFF} were calculated from I vs. V curves. Infrared spectra were recorded with Bruker Vertex 70 spectrophotometer, by using KRS-5 (4 mm) windows in transmittance mode in the range 4000−400 cm^{-1}; spectra were also acquired in attenuated

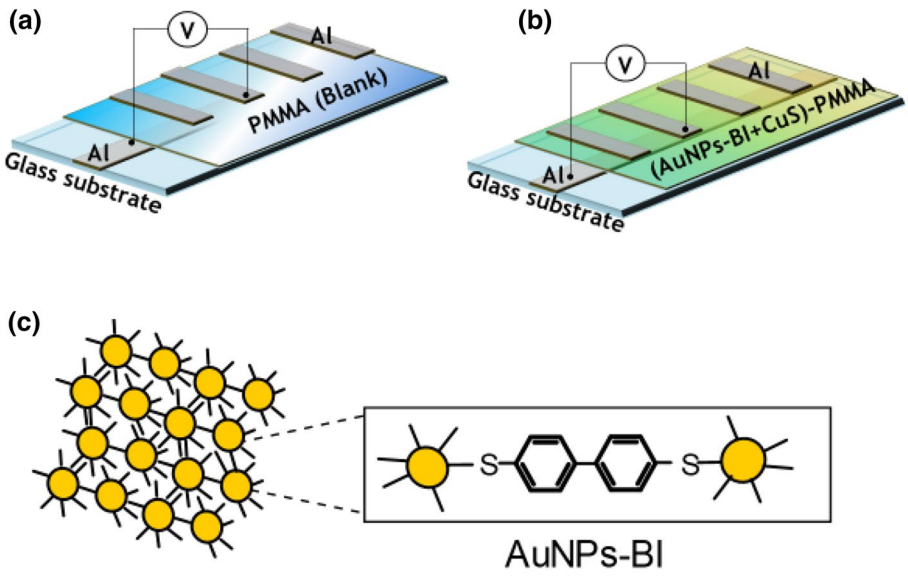

Fig. 1 Schematic representation of the **a** blank device based just on a compact layer of PMMA as storage layer, and representation of **b** the working WORM memory based on the CuS + AuNPs-BI blend in PMMA. Structure of AuNPs and biphenyl group **(c)**. The round gold nanoparticles are bound together by the thiol group (S) of the ligand [20]

total reflection mode (ATR) in the range 4000–600 cm^{-1}. UV–Vis spectra were recorded with a Cary 100 Varian spectrophotometer. All spectra were collected in the 190–900 nm range, with a 1 nm resolution, either from DCM solution with quartz cells with a 1 cm optical path and as thin films cast deposited on a quartz slide. FESEM images were acquired with an Auriga Zeiss instrument on drop-casted samples.

3 Results and discussion

In our previous work, we have synthesized and characterized the AuNPs-BI. As reported, the UV–Vis measurements showed the presence of LSPR band in the visible range 540–600 nm, typical of interconnected systems nanoparticles. Morphological characterization carried out with FESEM technique revealed a diameter of the as-synthesized AuNPs-BI of about 5–10 nm. At the same time, SR-XPS measurements confirmed the occurred functionalization of the metal surface in which Au atoms chemically interact with thiols end-groups of BI [28].

The electrical characterization of the samples was performed by cyclic voltammetry (CV) with applied voltages up to 9 V between the top and bottom Al electrodes. Figure 2a shows the voltage scan on the sample PMMA/AuNPs-BI/CuS, with voltage range ± 1.0 V. As a comparison the behavior of PMMA matrix was studied (see Fig. 2c), together with PMMA blended with AuNPs-BI and PMMA blended with CuS in the range ± 9.0 V. When AuNPs-BI or CuS were blended with PMMA, an immediate activation occurs, and the insulating PMMA matrix changed its state into a conductive one. In particular, in the case of PMMA/CuS the increase in conductivity was observed at 6 V and our interest was then focused on the PMMA/AuNPs/CuS blend.

In that moment the device is in the off-state (virgin) and shows an hysteresis, a typical capacitive characteristic [13], also visible when plotted in log scale (Fig. 2e). The I vs. V curve starts at the origin and the device starts to store charge and crosses the Y-axis with a current value in the order of 1 nA. However, when the voltage sweep is extended up to + 6.0 V, as shown in Fig. 2b, the extent of accumulated charges is increased, which increases significantly the electrical current above 3.0 V due to the formation of permanent conductive channels which set the device to on-state through the "writing" process. Figure 2e shows the device prior and after the writing process shown in Fig. 2b. Considering the voltage + 0.25 V as a reference of "reading" voltage, the current value was 1.2×10^{-9} A in the off-state, while, after the device is set into on-state by applying up to 6 V, the current reaches 4.1×10^{-4} A, or current density of 5×10^{-2} A·cm^{-2} at 1V, yielding an on-off ratio of 3.4×10^{5}. Figure 2d presents the slopes referring to the relation between I and V, which helps the understanding of the charge emission mechanisms that occur in the device under the different operations. The slope = 0.5 ($I \propto V^{0.5}$) at HRS indicates the device operates through Schottky [31] and Poole-Frenkel [32] emissions in the off-state, through defects inserted by the NPs. Once the applied voltage crosses the threshold to set the device into on-state (V_{set} = 3 V), an avalanche of electrons ($I \propto V^{17.0}$) are bridged between the AuNPs-BI and CuS NPs in the polymeric matrix as a result of a rapid and exponential growth of the trap-filling process of injected charge carriers [33], resulting in the ballistic transport of the charge carriers in the as-formed channel. The device operates at Ohmic regime ($I \propto V^{1.0}$) and hence the stable and continuous channel is formed [31, 33]. The on-state is retained over the

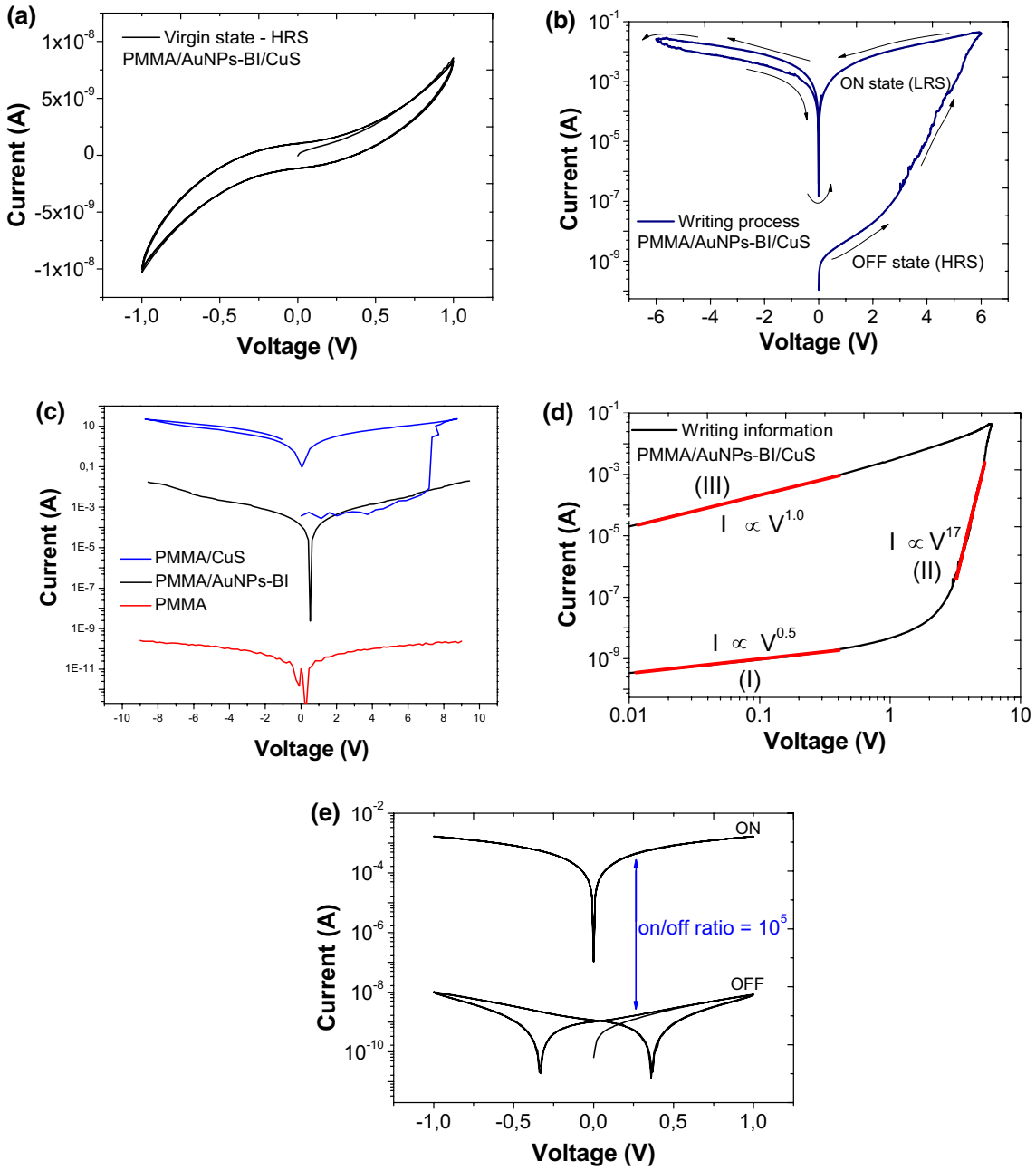

Fig. 2 Cyclic voltammetry of a WORM based on PMMA/AuNPs-BI/CuS blend. The measurements were performed from 0.0 V up to **a** ± 1.0 V for the reading operation in off-state, and **b** ± 6.0 V for the writing process. **c** Cyclic voltammetry of PMMA compared with PMMA/AuNPs-BI and PMMA/CuS blends. **d** Log(I) vs. Log(V) plot of the positive region of **c**. Inset of **a** presents the blank sample with PMMA as storage layer to show the absence of resistive switching in the sample without NPs, even at higher voltages (+9.0 V). **e** Plot of the off-state and on-state, respectively, before and after the writing process in (**c**). Reading sweep voltage performed at 1 V

time and the device is irreversibly written, which means the written information cannot be erased. Reading tests were performed after 30 days to show the endurance of the device.

For comparison with devices based on PMMA/AuNPs-BI/CuS, inset of Fig. 2a shows the application of up to 9 V on the blank sample, with only PMMA as active layer. The result shows that the pristine PMMA remains at HRS when high electric field is applied, with no presence of memory behavior.

According to latter literature results, CuS nanoparticles embedded into a polymeric network have shown a strong effect in formation mechanism of the conducting channel in composite polymer-nanoparticle memristor. As confirmed by V. Perla et al. [34], the role of the CuS semiconducting

nanoparticle is to make available intermediate energy levels which stabilize the conducting channels, defining a narrower voltage window for the ON/OFF transition. As a matter of fact, the composition of the active layer influences the whole performance of the memory device. As the AuNPs-BI works on the formation of the conductive channel within the PMMA, a further study about different concentrations of the NPs and their relationship with the WORM properties shall be considered in a future work.

In order to characterize the thin films, UV–Vis and FTIR spectra were acquired for the studied blends, before and after the writing process. In the case of PMMA/AuNPs-BI/CuS film, the UV–Vis spectrum evidenced the presence of a broad plasmonic resonance at about 670 nm with a red shift with respect to the pristine AuNPs-BI, as reported in Fig. 3a. FESEM study confirmed the small size of pristine AuNPs, with diameters below 10 nm (see Fig. 3b) as observed in our previous work [28]. ATR studies on the composite PMMA/AuNPs-BI/CuS before the writing process, reported in Fig. 3c, evidenced the bands of the functional groups due to the PMMA matrix (i.e., 1730 cm^{-1} and 1149 cm^{-1} due to C = O stretching of the ester and C–O–C), together with the bands centered at 2952 cm^{-1} and 2939 cm^{-1} attributable to C–H sp^3 stretching vibrations derived from alkyl chain of PMMA. The presence of AuNPs-BI can be envisaged in the 1450–1600 cm^{-1} region that contains the C–C sp^2 stretching vibrations of the biphenyl aromatic ring and with the bands located around 1084 and 752 cm^{-1}, associated with the in-plane C–H bending and the C–H out-of-plane of dithiobiphenyl functionalized AuNPs. After the writing process, the disappearance of the band of acrylate carboxyl group around 1730 cm^{-1} occurs, probably due to a reticulation process of the polymeric chains.

4 Conclusions

We hereby proposed a WORM device based on polymer PMMA blended with AuNPs-BI and CuS nanoparticles for non-volatile memory storage applications. Our experiments demonstrated that the information can be permanently written in the device at voltages higher than $V_{set} = 3$ V. The electrical resistance transition occurs, probably due to the formation of conducting channels through the NPs bridging inside the polymer. The presence of both AuNPs-BI and CuS lead to the formation of stable conductive channel whose stability remained after 30 days. One of the main limits could be the devices size which could negatively influence the switching speed of the device as well as the power needed to switch on and off the memory cell. In a future work, the devices will be miniaturized to study the transition-speed, as well as different concentrations of the NPs and their role in the WORM characteristics will be analyzed.

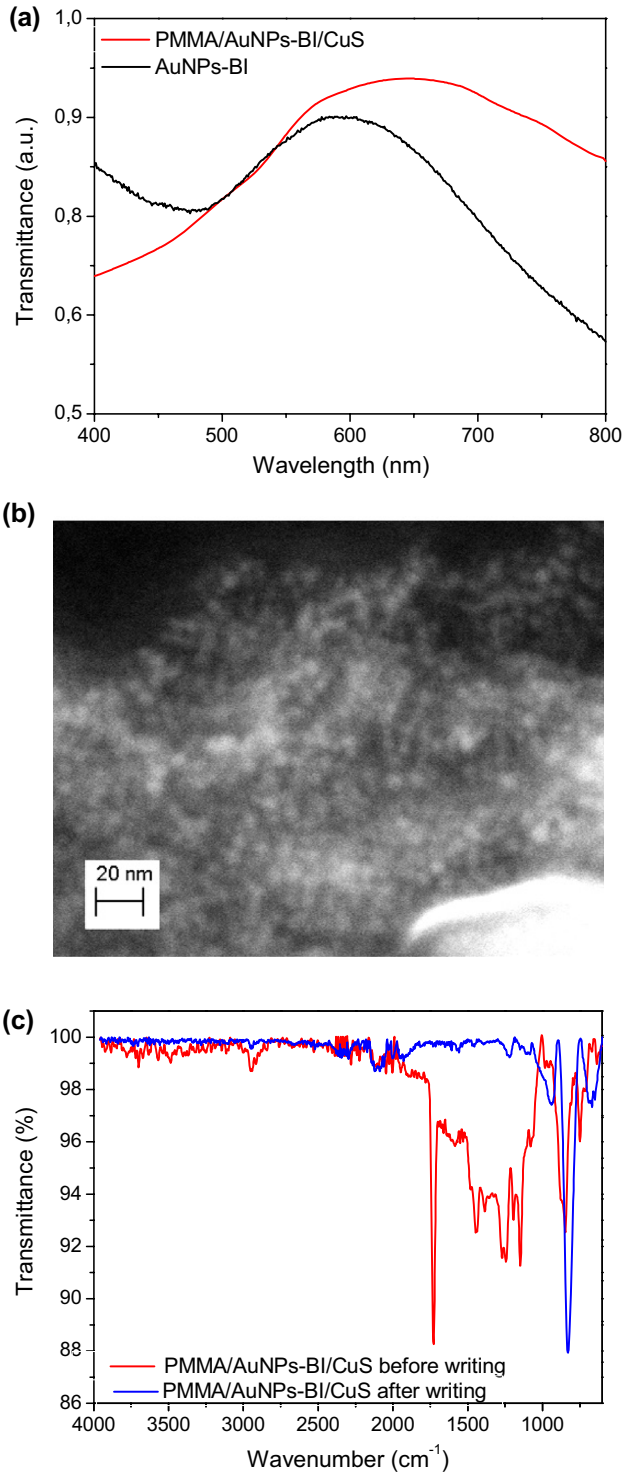

Fig. 3 UV–Vis spectra of pristine AuNPs-BI and AuNPs-BI/CuS films in PMMA on glass substrates **(a)**. Scanning electron microscopy image of a typical sample of AuNPs-BI **(b)**. ATR-FTIR spectra of a virgin sample (red line) and the same sample after the writing process (blue line) **(c)** (Color figure online)

Acknowledgements This work was supported by FAPESP (proc: 2013/07396-7; 2017/20809-0); PNPD/CAPES, CAPES 024/2012 Pro-equipamentos; Department of Chemistry, University of Rome Sapienza and Project "Torno Subito 2017" supported by Lazio Region of Italy, with FSE (Fondo sociale europeo, ID code: 9266). Ateneo Sapienza 2017 and 2019 grants are acknowledged.

References

1. S. Möller, C. Perlov, W. Jackson, C. Taussig, S.R. Forrest, Nature **426**, 166 (2003)
2. L. Chua, IEEE Trans. Circuit Theory **18**, 507 (1971)
3. D.B. Strukov, G.S. Snider, D.R. Stewart, R.S. Williams, Nature **453**, 80 (2008)
4. T.D. Dongale, S.S. Shinde, R.K. Kamat, K.Y. Rajpure, J. Alloys Compd. **593**, 267 (2014)
5. R. Waser, M. Aono, Nat. Mater. **6**, 833 (2007)
6. Y. Yang, S. Choi, W. Lu, Nano Lett. **13**, 2908 (2013)
7. J. Borghetti, G.S. Snider, P.J. Kuekes, J.J. Yang, D.R. Stewart, R.S. Williams, Nature **464**, 873 (2010)
8. D.B. Strukov, K.K. Likharev, Nanotechnology **16**, 888 (2005)
9. T. Ohno, T. Hasegawa, T. Tsuruoka, K. Terabe, J.K. Gimzewski, M. Aono, Nat. Mater. **10**, 591 (2011)
10. M.D. Pickett, G. Medeiros-Ribeiro, R.S. Williams, Nat. Mater. **12**, 114 (2013)
11. T. Driscoll, J. Quinn, S. Klein, H.T. Kim, B.J. Kim, Y.V. Pershin, M. Di Ventra, D.N. Basov, Appl. Phys. Lett. **97**(9), 093502 (2010)
12. S. Smith, S.R. Forrest, Appl. Phys. Lett. **84**(24), 5019–5021 (2004)
13. I.A. Hümmelgen, N.J. Coville, I. Cruz-Cruz, R. Rodrigues, J. Mater. Chem. C **2**(37), 7708–7714 (2014)
14. J. Fang, Q. Wang, X. Yue, G. Wang, Z. Jiang, High Perform. Polym. **28**, 1183 (2015)
15. J.C. Scott, L.D. Bozano, Adv. Mater. **19**, 1452 (2007)
16. D.V. Talapin, J.S. Lee, M.V. Kovalenko, E.V. Shevchenko, Chem. Rev. **110**, 389 (2010)
17. L.D. Bozano, B.W. Kean, M. Beinhoff, K.R. Carter, P.M. Rice, J.C. Scott, Adv. Funct. Mater. **15**, 1933 (2005)
18. S. Gao, X. Yi, J. Shang, G. Liu, R.W. Li, Chem. Soc. Rev. **48**(6), 1531–1565 (2019)
19. A. Dass, N.A. Sakthivel, V.R. Jupally, C. Kumara, M. Rambukwella, ACS Energy Lett. **5**, 207–214 (2019)
20. L. Fontana, I. Fratoddi, I. Venditti, D. Ksenzov, M.V. Russo, S. Grigorian, Appl. Surf. Sci. **369**, 115–119 (2016)
21. K. Reddy, K. Lee, A. G.-J. of nanoscience and, and undefined 2007, Ingentaconnect.Com (n.d.)
22. K.R. Reddy, B.C. Sin, K.S. Ryu, J.C. Kim, H. Chung, Y. Lee, Synth. Met. **159**, 595 (2009)
23. K.R. Reddy, B.C. Sin, C.H. Yoo, D. Sohn, Y. Lee, J. Colloid Interface Sci. **340**, 160 (2009)
24. K. Reddy, B. Sin, C. Yoo, W. Park, K. Ryu, J. L.-S. Materialia, and undefined 2008, Elsevier (n.d.)
25. M. Congiu, L.G.S. Albano, O. Nunes-Neto, C.F.O. Graeff, Electron. Lett. **52**(22), 1871–1873 (2016)
26. L.S.R. Rocha, A.Z. Simões, J.A. Cortés, M.A. Ramirez, F. Moura, C.R. Foschini, R. Tararam, M. Cilense, E. Longo, and C. O. Paiva-Santos, in *Magn. Ferroelectr. Multiferroic Met. Oxides* (Elsevier, 2018), pp. 275–282
27. M. Congiu, (2018)
28. L. Fontana, M. Bassetti, C. Battocchio, I. Venditti, I. Fratoddi, Colloids Surfaces A Physicochem. Eng. Asp. **532**, 282 (2017)
29. M. Brust, M. Walker, D. Bethell, D.J. Schiffrin, R. Whyman, J. Chem. Soc. Chem. Commun. **0**, 801 (1994)
30. M. Basu, A.K. Sinha, M. Pradhan, S. Sarkar, Y. Negishi, T. Pal, Environ. Sci. Technol. **44**, 6313 (2010)
31. E.Y.H. Teo, Q.D. Ling, Y. Song, Y.P. Tan, W. Wang, E.T. Kang, D.S.H. Chan, C. Zhu, (2006) Org Electron. Physics, Mater. Appl. 7(3): 173-180
32. M.H. Boratto, M. Congiu, S.B.O. dos Santos, L.V.A. Scalvi, Ceram. Int. **44**(9), 10796 (2018)
33. J. Wang, C. Youtsey, R. McCarthy, R. Reddy, N. Allen, L. Guido, J. Xie, E. Beam, P. Fay, Appl. Phys. Lett. **110**(17), 173503 (2017)
34. V.K. Perla, S.K. Ghosh, K. Mallick, Mater. Adv. (2020)